fNIRS – Hair density effect over NIRS signal

Methodological study of hair density effect over NIRS signal acquired during motor imagery task

Group 21

***Abstract*—Functional near-infrared spectroscopy (fNIRS), despite its advantages, presents challenges related to hair interference. This study investigates blood oxygenation level dependent (BOLD) response during motor imagery task and hair density effect over near-infrared spectroscopy (NIRS) signal. To conduct this analysis, the variation of hemoglobin concentration of 28 subjects was calculated from provided data. Signals were filtered and segmented, baseline-corrected and grouped according to hair density of subjects. The peak values of the motor cortex's channels were averaged and statistically compared using Student's *t*-test. The results obtained not only underscored a statistical disparity in signals between subjects with different hair densities, specifically in the motor cortex, but also highlighted how the difficulty of the motor imagery task, coupled with the chosen technique, contributes to substantial variability in signals, making their analysis challenging.**

***Keywords*—Blood oxygenation level dependent (BOLD) response, functional near-infrared spectroscopy (fNIRS), hair density, motor imagery.**

I. Introduction

Functional near-infrared spectroscopy (fNIRS) is a popular optical imaging technique widely used to investigate blood oxygenation level dependent (BOLD) response. This response occurs subsequently to the execution of one among motor, breath modification and cognitive tasks. Despite a low spatial resolution, fNIRS presents quite important advantages compared to other blood flow measurement technologies such as being non-invasive, relatively easy to use, portable and low cost [1], [2].

Recently, in scientific field the interest in this technique increased even more because it can be essential not only for basic research in neuroscience, but also for applications in medicine to improve the quality of life of post-traumatic and post-stroke patients using brain-computer interfaces (BCIs) for rehabilitation or to control prostheses and exoskeletons [2]. For this reason, it is important to focus on the acquisition of the fNIRS signals trying to obtain the highest quality possible. One of the main causes of artifacts and noise is the presence of hair at the interface between electrodes and scalp [3], [4].

The primary goal is to highlight whether there is a significant difference in signals acquired from subjects with different hair density during a motor imagery (MI) task [5]. However, a previous investigation to discern variations in neural activity within specific regions, during diverse behavioral states, is needed.

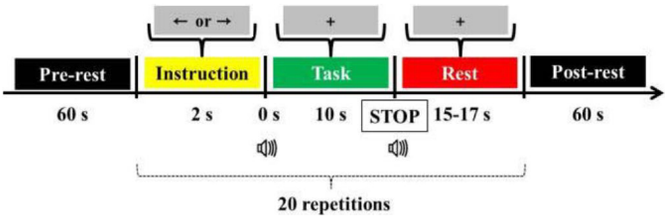

Fig. 1. Schematic sequence diagram of the experimental paradigm. Each session comprised a 1 min pre-experiment resting period, 20 repetitions of the given task and a 1 min post-experiment resting period. The task started with 2 s of a visual introduction of the task, followed by 10 s of a task period and resting period which was given randomly from 15 to 17 s. At the beginning and end of the task period, a short beep (250 ms) was played [6].

II. Materials and Methods

Data were provided by [6], as well as details about the acquisition and experimental procedure.

A. Subjects

Twenty-nine individuals with known health brain-related conditions were enlisted to participate in the experiment. Of the participants, twenty-eight were right-handed adults, while only one was left-handed (subject 13). The sample comprised 16 females and 13 males, with an average age of 28.4 ± 3.8 years (mean ± standard deviation). All subjects were naive to the MI experiment.

B. Data acquisition

Near-infrared spectroscopy (NIRS) data was collected in an ordinary bright room at 10 Hz sampling rate by NIRScout (NIRx GmbH, Berlin, Germany). Each adjacent pair of a source and a detector formed one physiological NIRS channel, called optode. A total of fourteen sources and sixteen detectors were strategically positioned, resulting in thirty-six physiological channels. Specifically, these channels were placed over frontal areas (nine channels around Fp1, Fp2, and Fpz), motor areas (twelve channels around C3 and C4), and visual areas (three channels around Oz). The distance between optodes was maintained at 30 mm. The optodes were placed according to the international 10-5 system. Adequate ambient light exclusion was achieved through secure contact between NIRS optodes and the scalp, complemented using an opaque cap. Continuous NIRS light intensity data were recorded at two distinct wavelengths: 760 nm and 850 nm.

C. Experimental procedure and task

In a well-lit room, 29 participants completed three sessions of alternating left- and right-hand MI (LMI and RMI). Each session consisted of a 1-minute rest period before and after the experiment, which was composed of 20 task repetitions with randomly alternating conditions between left- and right-hand.

Each repetition comprised a 2-second visual cue, 10-seconds imagery, and randomly assigned rest period lasting 15-17 s, marked by short beeps. Imagery involved haptic sensations of grabbing a ball, guided by visual cues at 1 Hz. Fig. 1 shows the schematic diagram of the experimental paradigm.

D. Data processing

All data processing was done using MATLAB R2023b (MathWorks, Natick, MA, USA).

First, the variations of oxygenated hemoglobin (ΔO_2Hb) and de-oxygenated hemoglobin (ΔHHb) concentration were calculated through the modified Beer-Lambert law. Starting from the system of two equations that follows

$$\begin{cases} \Delta A_{\lambda_1} = d \cdot B \cdot \left(\alpha_{\lambda_1}^{O_2Hb} \cdot \Delta O_2Hb + \alpha_{\lambda_1}^{HHb} \cdot \Delta HHb \right) \\ \Delta A_{\lambda_2} = d \cdot B \cdot \left(\alpha_{\lambda_2}^{O_2Hb} \cdot \Delta O_2Hb + \alpha_{\lambda_2}^{HHb} \cdot \Delta HHb \right) \end{cases} \quad (1)$$

the following matrix system has been solved:

$$\begin{bmatrix} \Delta A_{\lambda_1} \\ \Delta A_{\lambda_2} \end{bmatrix} = d \cdot B \cdot \begin{bmatrix} \alpha_{\lambda_1}^{O_2Hb} & \alpha_{\lambda_1}^{HHb} \\ \alpha_{\lambda_2}^{O_2Hb} & \alpha_{\lambda_2}^{HHb} \end{bmatrix} \begin{bmatrix} \Delta O_2Hb \\ \Delta HHb \end{bmatrix} \quad (2)$$

Since only signals proportional to ΔA with (V) unit measure were provided, it was used a correction factor of $1\ V^{-1}$ to obtain ΔA. d is the distance between the emitter and the detector. A value of 5.97 was used as the differential path length factor B for the brain tissue. Common Average Referencing (CAR) spatial filtering was employed to enhance the quality of the acquired signals. This technique involved subtracting the average value across all channels at each acquisition time, effectively eliminating global spatial trends from the data. The primary objective was to reduce potential noise and improve the reliability of subsequent analyses. Following CAR, two frequency filters were applied to the data in cascade. A low-pass filter with a cutoff frequency of 0.1 Hz was utilized to eliminate high-frequency instrument noise and systemic physiological noise, including signals associated with heart rate and respiration. A 0.01 Hz high-pass filter was implemented to remove baseline drifts, ensuring a cleaner representation of the underlying neural activity [7]. Both filters used are fourth-order Infinite Impulse Response (IIR) Butterworth filter. Given that IIR filters are characterized by phase distortion not easily predictable a priori, a double-pass filtering was implemented for each filter (zero-phase shift anticausal filter). The dataset was then segmented based on the distinct tasks involving either the right or left hand. This segmentation allowed a detailed exploration of neural responses specific to each task, covering a period from −5 to +25 s (relative times are referred to the task onset). This time frame included 3 s of pre-rest, 2 s of instructional cues, 10 s of task execution, and 15 s of rest. Such meticulous segmentation facilitated a comprehensive examination of temporal dynamics throughout the experimental timeline. To standardize the data and mitigate potential artifacts, a baseline correction was implemented. The value calculated averaging each epoch signal from −5 to −2 s was subtracted from the entire signal, ensuring that it started approximately from zero. It is noteworthy that, due to the limited representativeness of left-handed subjects in the study, with only one participant falling into this category, their data was excluded from the analysis to maintain a more homogeneous and representative dataset. Subsequently, the signals were averaged across sessions (10 epochs), and the maximum concentration value of oxygenated hemoglobin was identified for each epoch. This process produced a distribution of 10 values for each subject. The temporal localization of these peaks values was conducted within a 15-second timeframe, starting from the onset moment. This temporal range was selected based on the knowledge that the hemodynamic response to the specific task would manifest within the specified window. Afterwards, the subjects were divided into two groups based on their hair density classification: the first group consisted of individuals with low and medium density (L, M), and the second group included those with high and very high density (H, VH). This classification was determined after carefully examining the dataset. Since there were only three subjects with low and four with very high hair density, it was decided to combine them with their neighboring classes to ensure they were not excluded from the study and to avoid losing valuable information. Within each of these two groups, the distributions of peak values were then averaged across different subjects. From the available channels, the three ones showing the highest response in the motor cortex on the contralateral hemisphere in respect of the hand performing the task were selected. Channels C5-C3, FC3-C3, and CP3-C3 were chosen for the left hemisphere, while channels FC4-C4, CP4-C4, and C6-C4 were chosen for the right one. A further average of the distributions was calculated among the three channels.

E. Statistical test

A statistical test (Student's *t*-test) was conducted for two independent samples (L-M and H-VH) for both LMI and RMI tasks to assess potential statistical differences in NIRS signals among patients exhibiting varying levels of hair density. It was assumed equal variances between samples (homoscedasticity), employed a unilateral approach, which considers significant deviation in only one direction, and fixed a significance level α to 0.05.

III. Results

A. Ideal subject

The signals of subject 15 averaged across the three sessions are shown in Fig. 2. After examining the entire dataset, this subject was selected as a representation of an ideal behavioral pattern because it showcases the expected hemodynamic response, in line with existing literature for this kind of task. The most significant observation about the plot relates to the contralateral hemisphere's response: the concentration of O_2Hb begins to rise at the onset event and reaches a peak within a 10-seconds range. The channel which deviates the most from this trend is the C1-FC1, exhibiting a slightly delayed peak compared to the others. Conversely, HHb remains relatively constant, displaying subtle fluctuations. Signals of the right-hemisphere motor cortex exhibit a considerable variability of activations and deactivations instead.

B. Evolution of hemodynamic response – Grand Average

Considering how the experimental paradigm is structured, an analysis of the neural activation changes between different sessions was performed. In Fig. 3 the evolution of the hemodynamic response across the three sessions is observable. It is important to notice that the same color map

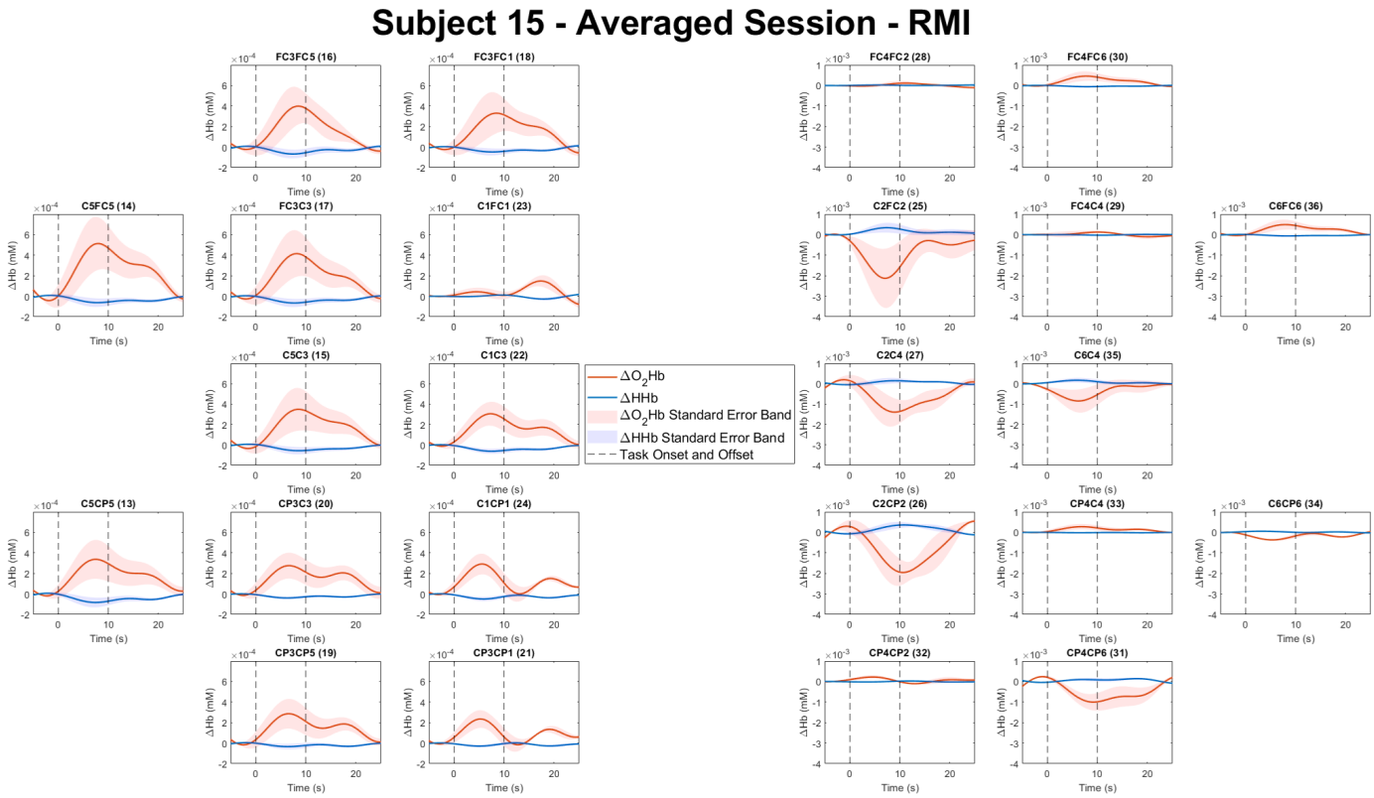

Fig. 2. Variation of oxygenated and de-oxygenated hemoglobin (ΔO_2Hb and ΔHHb) concentration in the motor cortex of subject 15 during right motor imagery. Signals are the mean of the averaged repetition over the three sessions. Each curve is paired with a shaded colored area representing the standard error band. The title of each subplot is composed by the name of the channel followed by the identification number between brackets. Different y-axis limits are set for left and right hemisphere channels to allow a clear visualization of the signals' dynamic.

limits are set for all the sessions allowing an immediate visual study of temporal evolution of BOLD response.

Firstly, it is clear the increase of activation of the contralateral motor cortex for both LMI and RMI. In particular, high values are found around C2-C4 and CP4-C4 for LMI, and around C5-FC5 for RMI in the last session. However, another high value is visible around channel C2-FC2. In addition to that of the motor cortex, it is noticeable an activation of the prefrontal cortex, very marked in the third session of RMI.

C. *Student's t-test*

Lastly, the implementation of the Student's *t*-test highlighted a statistical difference in peak amplitude of O_2Hb between the two subgroups (L-M and H-VH hair density). In particular, the *p*-value for LMI is equal to 5×10^{-5}, while for RMI is 0.003. The mean values of the peak distributions are displayed in the bar diagram in Fig. 4.

IV. Discussion

A. *Comparison between subjects*

As previously mentioned, the plot in Fig. 2 illustrates the ideal trend of the hemodynamic response (subject 15). This could be attributed to the fact that the subject was able to perform the task correctly, despite its complexity. Concerning the other subjects, the trends of HHb and O_2Hb exhibited significant variability compared to the expected ideal pattern. However, this variability is a well-known characteristic of this type of signal, and its causes can be diverse: even if O_2Hb increase is often considered a marker of neuronal activation, it can also be influenced by factors like changes in blood pressure or skin blood volume [8]. Moreover, certain subjects showed an early activation preceding the task onset. This phenomenon is likely attributed to subjects concentrating on the task before its start. In other cases, certain subjects exhibited a sustained rise in O_2Hb even after the task period, with the signal failing to return to baseline. Short intervals between repetitions risk overlapping distinct hemodynamic responses, suggesting a

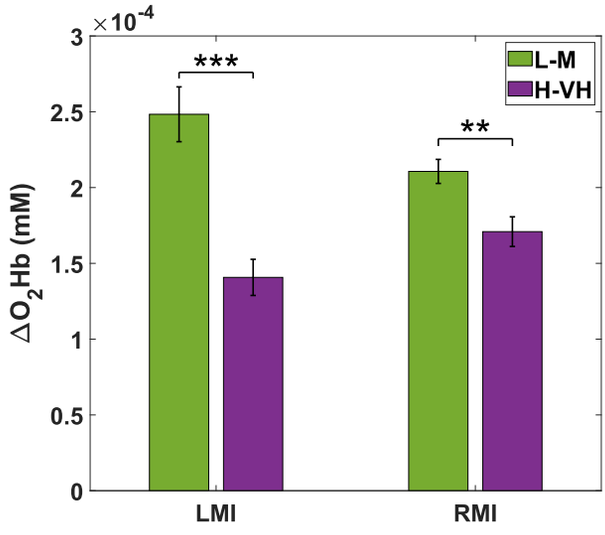

Fig. 4. Bar diagram showing the mean values of the oxygenated hemoglobin concentration peak distributions, calculated between subjects with low and medium hair density (L-M) and subjects with high and very high one (H-VH), for both left and right motor imagery. A standard error bar is displayed for each bar. Degree of significance of Student's *t*-test is shown through asterisks ($*$ if $0.01 \leq p < 0.05$, $**$ if $0.001 \leq p < 0.01$, $***$ if $p < 0.001$) positioned over pair of bars.

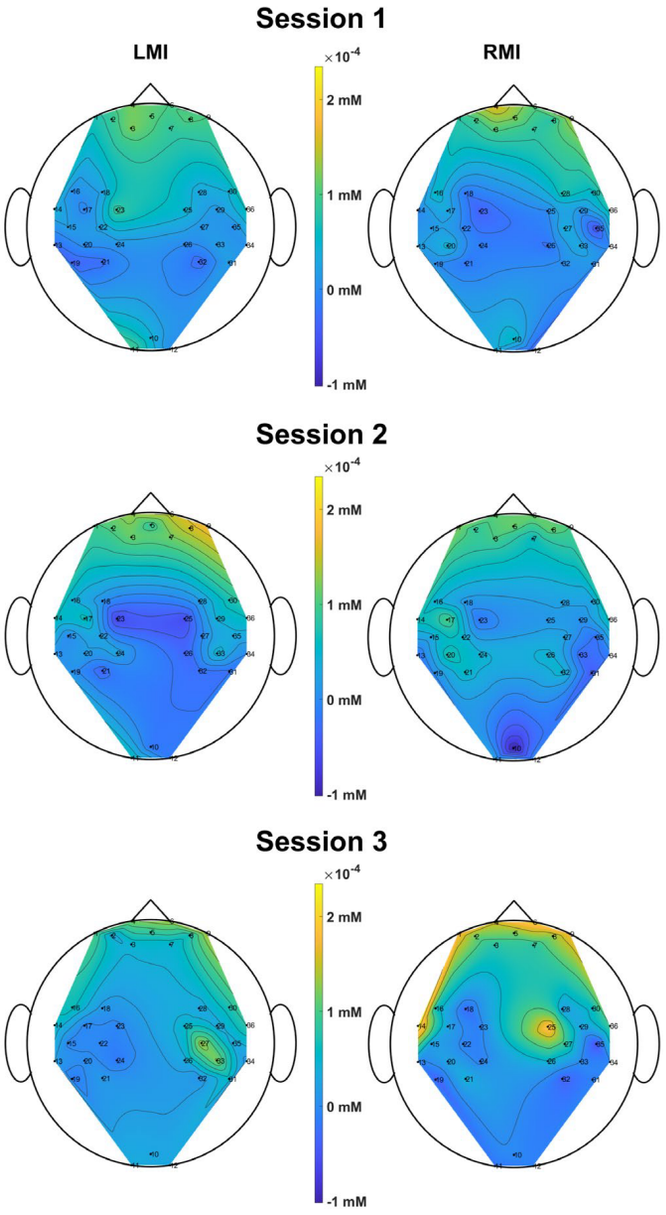

Fig. 3. Scalp evolution of grand average through the three sessions during right and left motor imagery. The color-coded topography represents the average values of the peak amplitudes within the task range. The numbers on the scalp indicate the channels, which are positioned on prefrontal, motor, and visual cortex. Crucial channels are: C5-FC5 (14), C2-FC2 (25), C2-C4 (27), and CP4-C4 (33).

potential utility in extending the rest period [6]. Furthermore, the possibility of other thoughts interfering with task-related cognition cannot be discarded. It is crucial to emphasize that signal quality depends not only on acquisition and data processing methods but is significantly influenced by the subject's ability to focus on the activity and their familiarity with it. Additionally, the proposal of using objective questionnaires has been suggested to assess the effectiveness of MI, and preliminary training may be necessary to reliably distinguish contralateral activations [6], [7].

B. Evolution of hemodynamic response – Grand Average

In Fig. 3 it is reported a topography showing the evolution of the signals over the three sessions.

Regarding the prefrontal cortex, for RMI it is possible to observe the peak of O_2Hb in the third session. This is probably caused by fatigue brought by the tough task that led the subjects to focus more and more on the assignment. The involvement of prefrontal areas in unfamiliar tasks aligns with their role in regulating cognitive functions such as attention, concentration, and movement planning [9]. An additional factor is related to the nature of MI tasks which can be broadly categorized into visual, involving self-visualization of movements, and kinesthetic, where individuals imagine the sensations produced by the movement. In a study conducted by Guillot et al., a comparison between kinesthetic and visual MI revealed that kinesthetic MI shares more analogous neural pathways with actual motor execution [7]. Concerning LMI there is a fluctuation in the prefrontal trend, probably the result of the involvement of the non-dominant hand in the execution of the task.

Numerous studies have widely discussed the similarities in the brain areas involved during motor execution and motor imagery [7]. These are the supplementary motor area (SMA), involved in planning movements based on remembered sequences of movements and coordinating bilateral movements, the premotor area (PMA), which has a role in organizing movements based on sensory information, for example a visual stimulus, and finally the posterior parietal cortex (PPC), important in planned movements, spatial reasoning, and attention [1], [2]. Knowing that allows to say that a common behavior is noticeable in the motor cortex: for both LMI and RMI, with session progress there is an activation in the hemisphere contralateral to the hand involved (around C2-C4 and CP4-C4 for LMI, and around C5-FC5 for RMI). This suggests the subjects become more proficient in activating the appropriate brain area over sessions. A noteworthy aspect of the plot is the bilateral activation, very pronounced in the last session of RMI, during which channel C2-FC2 reaches almost the same activation of the channel C5-FC5. This may be associated with the inherent difficulty of motor tasks, leading to challenges in distinguishing the sensation between right and left MI. Furthermore, this is plausibly also due to a residual activation from the previous task [7].

C. Hair density effect

To carry out the statistical analysis, it was decided to use the signals averaged across the three sessions to mitigate the above-mentioned problems characterizing each of them and to fully exploit the information contained within the entire dataset.

The bar diagram in Fig. 4, reporting the Student's *t*-test results, first illustrates a statistical difference between O_2Hb signals from L-M and H-VH hair density groups for both LMI and RMI. Additionally, the L-M signals exhibit a higher mean of the maximum peak amplitude values compared to H-VH signals. This outcome was expected, given that hair represents an obstacle to the photon pathway, and an increase in follicle density should theoretically reduce photon penetration into the scalp. This observation aligns with previous studies, which also suggest that higher follicle density contributes to an attenuation of the measured O_2Hb value. Thick and voluminous hair may also prevent the adhesion between the optode-helmet and the skin [3], resulting in elevated photons scattering and absorption.

Because hair significantly impacts on NIRS, various solutions were proposed in the literature. For instance, certain

studies, such as [10], opted to focus on the prefrontal cortex or to select subjects with low hair density to mitigate these challenges. Moreover, Bilal Khan et al. tackled this issue by innovatively developing brush optodes for fNIRS [4]. This solution aims to enhance optical contact with the scalp, providing an effective means to mitigate the interference posed by hair during this kind of studies.

REFERENCES

[1] N. Iso *et al.*, "Hemodynamic Signal Changes During Motor Imagery Task Performance Are Associated With the Degree of Motor Task Learning," *Front Hum Neurosci*, vol. 15, 2021, doi: 10.3389/fnhum.2021.603069.

[2] A. E. Hramov, V. Grubov, A. Badarin, V. A. Maksimenko, and A. N. Pisarchik, "Functional Near-Infrared Spectroscopy for the Classification of Motor-Related Brain Activity on the Sensor-Level," *Sensors*, vol. 20, no. 8, 2020, doi: 10.3390/s20082362.

[3] J. Kwasa *et al.*, "Demographic reporting and phenotypic exclusion in fNIRS," *Front Neurosci*, vol. 17, 2023, doi: 10.3389/fnins.2023.1086208.

[4] B. Khan *et al.*, "Improving optical contact for functional near-infrared brain spectroscopy and imaging with brush optodes," *Biomed. Opt. Express*, vol. 3, no. 5, pp. 878–898, May 2012, doi: 10.1364/BOE.3.000878.

[5] M. A. McIntosh, U. Shahani, R. G. Boulton, and D. L. McCulloch, "Absolute Quantification of Oxygenated Hemoglobin within the Visual Cortex with Functional Near Infrared Spectroscopy (fNIRS)," *Invest Ophthalmol Vis Sci*, vol. 51, no. 9, pp. 4856–4860, Sep. 2010, doi: 10.1167/iovs.09-4940.

[6] J. Shin *et al.*, "Open Access Dataset for EEG+NIRS Single-Trial Classification," *IEEE Transactions on Neural Systems and Rehabilitation Engineering*, vol. 25, no. 10, pp. 1735–1745, 2017, doi: 10.1109/TNSRE.2016.2628057.

[7] A. M. Batula, J. A. Mark, Y. E. Kim, and H. Ayaz, "Comparison of Brain Activation during Motor Imagery and Motor Movement Using fNIRS," *Comput Intell Neurosci*, vol. 2017, p. 5491296, 2017, doi: 10.1155/2017/5491296.

[8] W.-L. Chen *et al.*, "Functional Near-Infrared Spectroscopy and Its Clinical Application in the Field of Neuroscience: Advances and Future Directions," *Front Neurosci*, vol. 14, 2020, doi: 10.3389/fnins.2020.00724.

[9] P. Pinti, M. F. Siddiqui, A. D. Levy, E. J. H. Jones, and I. Tachtsidis, "An analysis framework for the integration of broadband NIRS and EEG to assess neurovascular and neurometabolic coupling," *Sci Rep*, vol. 11, no. 1, p. 3977, 2021, doi: 10.1038/s41598-021-83420-9.

[10] X. Fang, B. Pan, W. Liu, Z. Wang, and T. Li, "Effect of Scalp Hair Follicles on NIRS Quantification by Monte Carlo Simulation and Visible Chinese Human Dataset," *IEEE Photonics J*, vol. 10, no. 5, pp. 1–10, 2018, doi: 10.1109/JPHOT.2018.2865427.